

Influences and Optimization of Electrical Discharge Machining Parameters for Improving Form Tolerances of Micro Hole on SiC Conductive Ceramic Composite

¹C.Murugan ²Dr. R. M. Satheesh Kumar

¹Research Scholar ²Professor & Head of the Department

¹PSY Engineering College, Sivagangai ²KLN College of Engineering, Sivagangai, Tamil Nadu, India

Abstract

Advanced Ceramics find wide range of industrial applications. Cutting of advanced ceramic (SiC) is very difficult using conventional machining methods due to its low fracture toughness. In the past few years, researchers have claimed successful machining of ceramic composites using EDM process. Furthermore, increasing trend, necessity of miniaturization, micro components in MEMS and semiconductor industry, micro mould and dies, furnace, micro injection, stamping, fuel nozzles, micro probes, photo-masks and micro tools. etc, have demanded the development of micro-machining methods for advanced ceramics. Therefore, this research was focused on micro hole drilling-EDM of SiC. The optimization of micro drilling in electrical discharge machining process parameters of SiC to improve the multiple performance characteristics such as, high material removal rate, low electrode wear, surface finish and accurate over cut was investigated and optimized by the Grey-Taguchi method. The influences of peak current, pulse on-time, pulse off-time and spark gap on electrode wear (EW), material removal rate (MRR), circularity(CIR), taper ratio(TR) and overcut (OC) in the micro drilling operation using EDM of SiC were analyzed. The experimental results show that high MRR, low TWR, accurate OC, better CIR, better TR under the micro drilling electrical discharge machining. Hence, it is clearly shown that multiple performance characteristics can be improved by using the Grey-Taguchi method.

Keyword- Sink EDM; electrode wear; material removal rate; over cut; CIR, TR, Grey-Taguchi method

I. INTRODUCTION

SiC based composites are well-recognized engineering materials for high temperature applications. Due to their high strength, low density, fracture toughness good electrical conductivity and high hardness, silicon-based composites are used in heat exchangers, non-ferrous molten metal handling, gas turbine components, wear-resistant components, and aircraft engines, among other applications. Because these materials have high hardness, conventional machining processes for the production of complex shapes are extremely difficult and expensive because machining may cause cracks on the exterior parts of the working materials. Thus, it is more suitable to select a non-traditional machining process for these experiments. EDM is a widely used non-traditional machining process that maintains good dimensional tolerance in electrically conductive materials despite the high strength and hardness of the materials. To incorporate better wear properties, electrically conductive particles, such as TiC, TiN, ZrB₂, and TiB₂, are reinforced with a Si₃N₄ matrix. The machine should work effectively on conductive electrical pieces regardless of their mechanical properties and shape spark eroding processes [1-4]. Sanchez et al. [5] developed optimum electro discharge machining technology for advanced ceramics and EDM proves its feasibility for the optimum machining of ceramics. The ceramic composites are manufactured by a hot pressing technique and the high-temperature sintering of powder metallurgy [6]. The ceramic composites should possess good electrical conductivity for their machining by the EDM. Recently, various special processes have been used to manufacture conductive ceramic-based composites [7]. Ahmad and Sueyoshi studied the outcome of the mechanical and electrical possession of silicon nitride and titanium nitride composites [2, 5, 8]. Their research used a hot pressing technique between 1250°C and 1350°C to prepare the experimental composites. Drawin et al. [9] used the same preparation technique as Ahmad and Sueyoshi. The research by Darwin et al. also incorporates the addition of silicon nitride composites to improve the MRR during the spark eroding process. The above mentioned research also demonstrated that conductive ceramic-based composites are being manufactured and used for an increasing number of applications. As an attempt to determine the most suitable electrode material, Muttamara et al. [10] used Cu, Cu-W and Ag-W as materials for the micro-EDM and suggested the Cu electrode as having the highest MRR, followed by the CuW and AgW electrodes. Dey et al. [11] also suggested that copper electrodes are suitable for achieving a high metal removal rate pertaining to the electrical discharge while machining ceramics.

Recently, the Taguchi technique has been used as an experimental methodology to minimize the number of trials based on experimental design. Precisely, an orthogonal array and the grey relational analysis are employed to achieve the optimal parameter combinations [12, 13]. Additionally, the Taguchi grey relational analysis (TGRA) and ANOVA are used to analyze the importance of machining parameters [3, 8]. Chiabert et al. [14] reviewed the current geometric tolerance theories and algorithms for inspection data analysis. In manufacturing engineering, EDM is becoming a vital process in the recent scenario due to the evolving trend of micro- and nano- applications. Therefore, precision components with good form tolerances are needed in EDM manufacturing. This experimental work focuses on analyzing the application of conventional EDM on micro scale feature machining, in silicon Carbide composites. A literature research indicated that few appreciable experimental works have been completed in this field. Moreover, form and orientation tolerances are relevant responses in non-conventional machining processes, such as EDM [15-22]. This article presents to optimize the EDM process parameters to improve the MRR, TWR, CIR, Dilation of hole, TR. Hyun-Kyu Yooa, Ji-HyeKoa, As the unit discharge energy increased, the debris size and its standard deviation for YN-SiC increased, while those of SUS304 decreased [23]. Mustafa Ay & Ulaş Çaydaş, studied micro-electrical discharge machining (EDM) drilling process of Inconel 718 nickel-based Super alloy with multi performance characteristics The hole taper ratio (Ht) and hole dilation (Hd) were the measured performances [24]. Krishna Kumar Saxena, n, Anand Suman Srivastava b analyzed that Micro EDM operation process parameters (Voltage, Capacitance and Threshold) affect the Surface Roughness, MRR, TWR and ROC significantly [25].

Hence, the process can be applied to close tolerance components, such as tools, dies, mould and press work operations, due to the improvement in the above response parameters. For example, in the application of extrusion die for manufacturing hard steel product, this extrusion die that are made by an EDM, which needs for circularity, over cut and taper ratio to accurate size and shape.

II. MATERIALS AND METHODS

The machine used for this work was the OSCARMAX spark EDM. Feed in the vertical direction was controlled by a servo drive. The dielectric fluid was the EDM oil solution, and the electrode suction flushing method was used. Removal of the debris generated during the machining process was required to maintain smooth processing during the electrical discharge machining; thus, a solid electrode was selected. Table.1 shows the operating conditions of the EDM machine (Model no: SD325-ZNC) shown in Fig.1, which is used to machine the composite material.

<i>Working conditions</i>	<i>Description</i>
<i>Electrode material</i>	<i>Electrode material Chromium Zirconium copper</i>
<i>Electrode Diameter</i>	<i>Ø 700 µm, length – 40 mm</i>
<i>Shape of Tool Electrode</i>	<i>Cylindrical shape</i>
<i>Electrode polarity</i>	<i>-ve</i>
<i>Work piece polarity</i>	<i>+ve</i>
<i>work material type</i>	<i>Silicon carbide</i>
<i>Work piece material size</i>	<i>Ø50 mm, thickness-2 mm</i>
<i>Type of current</i>	<i>DC Power Supply</i>
<i>Dielectric fluid</i>	<i>EDM oil</i>

Table 1: EDM operating conditions

A. Process Variables and their Levels of Spark EDM

<i>Symbol</i>	<i>Parameter</i>	<i>Units</i>	<i>Level</i>	<i>Level 2</i>	<i>Level 3</i>
<i>A</i>	<i>Current</i>	<i>A</i>	<i>5</i>	<i>4</i>	<i>2</i>
<i>B</i>	<i>Pulse On time</i>	<i>µs</i>	<i>15</i>	<i>10</i>	<i>6</i>
<i>C</i>	<i>Pulse off time</i>	<i>µs</i>	<i>22</i>	<i>15</i>	<i>10</i>
<i>D</i>	<i>Dielectric pressure</i>	<i>Kg/cm²</i>	<i>15</i>	<i>16</i>	<i>17</i>



Fig. 1: OSCARMAX Spark EDM machine

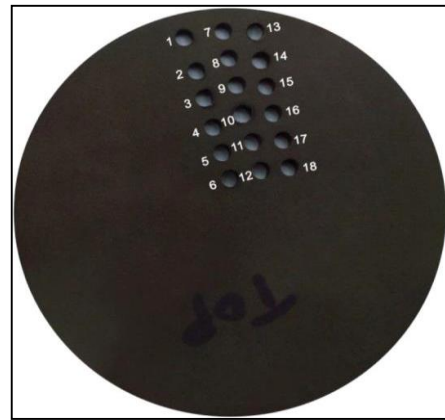


Fig. 2: shows micro holes in machined work piece

The work piece material was hot-pressed SiC, a composite-grade developed as an electrically conductive ceramic. The work piece was a disc with a 50 mm diameter and 2 mm thickness. A copper-based electrode composed of Cr-Zr - Cu in the form of a rod with a 0.7 mm diameter and a 100 mm length was used to achieve a higher MRR [10]. Taguchi developed a method for DOE that reduces the number of experiments and analyses required to achieve proper outcomes [15–20]. In this work, SiC can be considered a specimen material. Being a powerful tool in parameter design, the experiment is designed using the Taguchi method. The MRR was calculated based on the weight difference of the work piece before and after undergoing the EDM process. The weights of the electrode and work specimen were measured using electronic weighing machine. The MRR was determined using Equation (1).

$$\text{MRR (g / min)} = \frac{V_a - V_b}{t} \quad (1)$$

Where V_b - weight of the specimen material before eroding (g), V_a - weight of the specimen material after eroding (g), Similarly, the TWR was determined using Equation (2)

$$\text{TWR (g / min)} = \frac{V_{tb} - V_{ta}}{t} \quad (2)$$

Where V_{tb} - weight of the electrode before eroding (g), V_{ta} - weight of the electrode after eroding (g), t - Machining time (min).

B. Calculation of Circularity

Circularity is defined as a condition of a surface of revolution (sphere, cone, and cylinder) where all points of the surface intersected by any plane perpendicular to a common axis (cone, cylinder) or passing through a common centre (sphere) are equidistant from the axis of the centre. The form tolerances and orientation tolerances were measured by Optical Profile Projector, model ZEISS Contoura G2, with an accuracy of 4.5µm. At least four measurements of circularity were taken for each hole and average (Fig. 1a). The circularity of drilled holes was calculated in terms of circularity (ΔC) by using the formula

$$\Delta C = (D_i - D_e) + \dots + (D_n - D_e) / 4$$

Where, $i=1,2,..,4$, n is the number of measurement.

1) Specification of optical Profile Projector



2) *Specifications:*

- Models : V30 Profile Projector
- Variable Intensity :24Vx150W
- Magnifications :10X,20X.25X.SOX,100x
- Dual Xenphot Light Source :24Vx150W
- MagnificationAccuracyContour:0.05%
- Surface :0.10%
- Screen : 360mm Dia
- Rotation : 360°

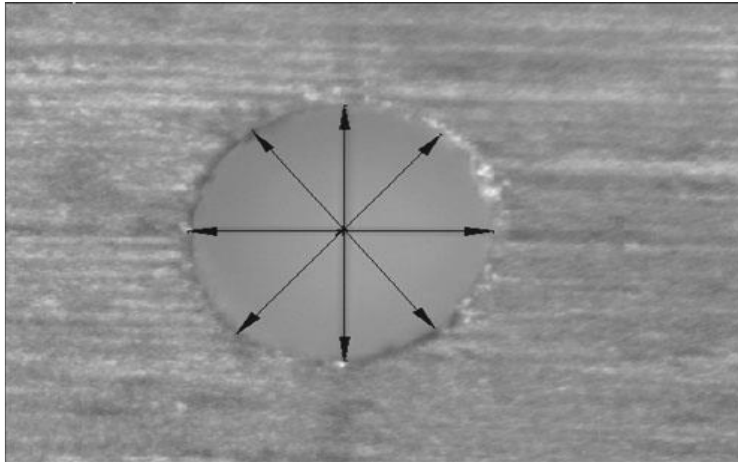


Fig. 1: a) Dimension were measured using optical profile projector

The dilation of holes (OC) was determined by the following equation:

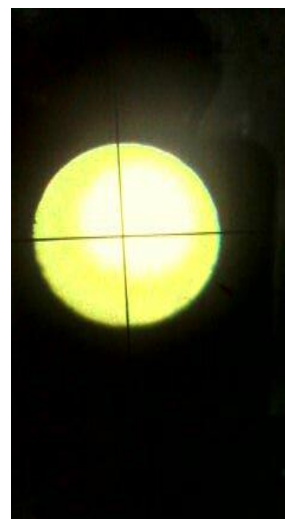
$$\text{Dilation of hole (Over Cut)} = D_{\max} - D_e$$

Where D_e is the original electrode diameter.

3) *Image Scanned By Optical Profile Projector*



Measurement at Entrance



Measurement at Exit

In EDM drilling, entry hole diameter is normally larger than exit hole diameter and thus the drilled holes are generally positively tapered.

The hole taper ratio (Ht) was calculated by using following formula:

$$\text{Taper Ratio} = \frac{D_{\text{entrance}} - D_{\text{exit}}}{2 \times \text{thickness of material}}$$

Where, D_{entrance} is the hole entrance diameter,

D_{exit} is the hole exit diameter and t is the thickness of the material.

L18 Orthogonal array with factors and responses.

Ex.no	Process parameter-Input parameter				Output parameter		Circularity (CIR)	Over Cut (Dilation)	taper ratio (TR)
	Current	Pulse On time	Pulse off time	Dielectric pressure	MRR	TWR			
	A	μs	μs	Kg/cm ²	g/min	g/min	mm	mm	mm
5	15	22	15	0.0036	0.0003	0.007	0.023	0.065	
5	10	15	16	0.0068	0.0011	0.025	0.031	0.055	
5	6	10	17	0.0185	0.0011	0.016	0.028	0.214	
4	15	22	16	0.0043	0.0004	0.009	0.023	0.047	
4	10	15	17	0.0050	0.0008	0.013	0.025	0.038	
4	6	10	15	0.0045	0.0006	0.011	0.018	0.092	
2	15	22	17	0.0069	0.0012	0.007	0.026	0.210	
2	10	15	15	0.0037	0.0003	0.010	0.019	0.125	
2	6	10	16	0.0021	0.0001	0.006	0.008	0.055	
5	15	22	16	0.0052	0.0009	0.019	0.026	0.045	
5	10	15	17	0.0059	0.0007	0.020	0.032	0.055	
5	6	10	15	0.0047	0.0013	0.004	0.050	0.098	
4	15	22	15	0.0058	0.0012	0.006	0.058	0.148	
4	10	15	16	0.0054	0.0008	0.007	0.030	0.180	
4	6	10	17	0.0029	0.0001	0.010	0.036	0.298	
2	15	22	17	0.0038	0.0008	0.009	0.022	0.598	
2	10	15	15	0.0023	0.0001	0.008	0.038	0.039	
2	6	10	16	0.0038	0.0004	0.002	0.010	0.175	

III. RESULTS AND DISCUSSION

The signal-to-noise (S/N) ratio for the relating experimental results is calculated via Equations (3) and (4). A higher S/N ratio is better:

$$S / N \text{ ratio } (\eta) = - 10 \log_{10} (1/n) \sum 1/ y_{ij}^2 \text{ ----- (3)}$$

Where, η = the resultant S/N ratio, n = the number of replications, k = number of experiments and y_{ij} = the observed response value, where $i = 1, 2, \dots, n$ and $j = 1, 2, \dots, k$. i is the response value in the j th experiment. i =number of responses and j =number of experiments. In this research, a higher MRR is advantageous. Therefore, Equation (3) is used to calculate the S/N ratio values of the MRR.

A lower S/N ratio is better:

$$S / N \text{ ratio } (\eta) = - 10 \log_{10} (1/n) \sum y_{ij}^2 \text{ ----- (4)}$$

Where, η = the resultant S/N ratio, n = the number of replications, and y_{ij} = the observed response value, where $i = 1, 2, \dots, n$ and $j = 1, 2, \dots, k$, i is the response value in the j th experiment. i =number of responses and j =number of experiments. Therefore, Equation (4) is used to evaluate the S/N ratio values of the experimental results. Normalization of the experimental data for each response is completed. Normalization is often considered a transformation that is carried out by individual data that is entered and can be circulated and measured by a greater analysis, where y_{ij} is normalized as X_{ij} ($0 \leq X_{ij} \leq 1$) by applying the equation. The normalization prevents the impact of choosing various components to decrease the variables and is mandatory in standardizing data when examining it with either Grey theory or another technique. Making an assessment of an array approximate to 1 can be deducted from the value of the same array. The receptiveness of the standard method in the outcome is also analyzed because the method of normalization changes the grades. Thus, the S/N ratio must be considered while normalizing the data in a GRA.

$$Y_{ij} - \min y_{ij} \text{ (} i= 1,2,\dots, n \text{)}$$

$$\text{-----S/N ratio in which a higher value is better (5) } \max Y_{ij} \text{ (} i= 1,2,\dots, n \text{)} - \min y_{ij}$$

$$\text{(} i= 1,2,\dots, n \text{)}$$

$$= \max Y_{ij} \text{ (} i= 1,2,\dots, n \text{)} - Y_{ij}$$

$$\text{-----S/N ratio in which a lower value is better (6)}$$

$$\max Y_{ij} \text{ (} i= 1,2,\dots, n \text{)} - \min y_{ij} \text{ (} i= 1,2,\dots, n \text{)}$$

In this work, to maximize the performance characteristics, the normalized values of the experimental results are obtained by Equation (5) and by minimizing the performance characteristics in Equation (6). The results are given in Table 4.

S.No	S/N Ratio					Normalising				
	MRR	TWR	CIR	OC	TR	MRR	TWR	CIR	Dilation	TR
	-8.82799	71.1067	38.4164	32.7654	23.7417	0.2532	0.4489	0.7094	0.5331	0.1948
	-43.2962	59.5545	32.0412	30.1728	25.1927	0.5447	0.9178	1.0000	0.6838	0.1342
	-34.6555	59.1617	35.9176	31.0568	13.3917	1.0000	0.9337	0.8233	0.6324	0.6271
	-47.2735	66.9791	34.4249	32.7654	26.5580	0.3351	0.6165	0.8913	0.5331	0.0771

	-46.0452	61.6082	37.7211	32.0412	28.4043	0.3999	0.8344	0.7411	0.5752	0.0000
	-46.9980	63.9000	39.1721	34.8945	20.7242	0.3496	0.7414	0.6750	0.4094	0.3208
	-43.2853	58.0925	43.0980	31.7005	13.5556	0.5453	0.9771	0.4960	0.5950	0.6203
	-48.7061	70.9850	40.0000	34.4249	18.0618	0.2596	0.4539	0.6372	0.4366	0.4320
	-53.6336	76.8609	44.4370	41.9382	25.1927	0.0000	0.2154	0.4350	0.0000	0.1342
	-45.7516	61.3146	34.4249	31.7005	26.9357	0.4153	0.8464	0.8913	0.5950	0.0613
	-44.6150	63.2034	33.9794	29.8970	25.1927	0.4752	0.7697	0.9117	0.6998	0.1342
	-46.4725	57.5293	47.9588	24.7314	20.1755	0.3773	1.0000	0.2744	1.0000	0.3438
	-44.7223	58.7017	44.4370	34.4249	16.5948	0.4696	0.9524	0.4350	0.4366	0.4933
	-45.3314	62.2333	43.0980	30.4576	14.8945	0.4375	0.8091	0.4960	0.6672	0.5644
	-50.6069	78.9064	40.0000	28.8739	10.5157	0.1595	0.1323	0.6372	0.7593	0.7473
	-48.5010	62.1859	40.9151	33.1515	4.4660	0.2704	0.8110	0.5955	0.5107	1.0000
	-52.9193	82.1672	41.9382	28.4043	28.1787	0.0376	0.0000	0.5489	0.7865	0.0094
	-48.3184	68.3184	53.9794	40.0000	15.1392	0.2801	0.5621	0.0000	0.1126	0.5541

Table 4: S/N ratio values and normalized S/N ratio values

Calculate the grey relational coefficient (GRC) in the normalization experimental results.

$$\gamma_{jk} = \frac{y_{kj} - \Delta_{\min}}{\Delta_{\max} + \xi(\Delta_{\max} - \Delta_{\min})} \quad (7)$$

The defined range of $0 \leq \xi \leq 1$ determines the differentiated coefficient. The GRG is determined using the following equation:

$$\gamma_j = \frac{1}{k} \sum_{i=1}^m \gamma_{ij} \quad (8)$$

Where γ_j = the grey relation rank for the j^{th} test and k = the number of output parameters. The values for the grey rank provided in Table 5 are plotted at Fig. 5.

Ex.No	Grey relational Co-efficient					Grey grade	Rank
	MRR	TWR	CIR	OC	TR		
	0.4010	0.4757	0.6324	0.5171	0.3831	0.4819	14
	0.5234	0.8588	1.0000	0.6126	0.3661	0.6722	2
	1.0000	0.8830	0.7389	0.5763	0.5728	0.7542	1
	0.4292	0.5659	0.8215	0.5171	0.3514	0.5370	11
	0.4545	0.7513	0.6588	0.5406	0.3333	0.5477	10
	0.4346	0.6591	0.606	0.4584	0.424	0.5165	13
	0.5237	0.9563	0.498	0.5525	0.5684	0.6198	5
	0.4031	0.4779	0.5795	0.4702	0.4682	0.4798	15
	0.3333	0.3892	0.4695	0.3333	0.3661	0.3783	18
	0.4610	0.7650	0.8215	0.5525	0.3475	0.5895	7
	0.4879	0.6847	0.8498	0.6248	0.3661	0.6027	6
	0.4454	1.0000	0.408	1.0000	0.4324	0.6572	3
	0.4852	0.9131	0.4695	0.4702	0.4967	0.5669	8
	0.4706	0.7237	0.498	0.6004	0.5344	0.5654	9
	0.3730	0.3656	0.5795	0.675	0.6643	0.5315	12
	0.4067	0.7257	0.5528	0.5054	1.0000	0.6381	4
	0.3419	0.3333	0.5257	0.7008	0.3354	0.4474	16
	0.4099	0.5331	0.3333	0.3604	0.5286	0.4331	17

Table 5: computing the grey relational rank values by the GRA.

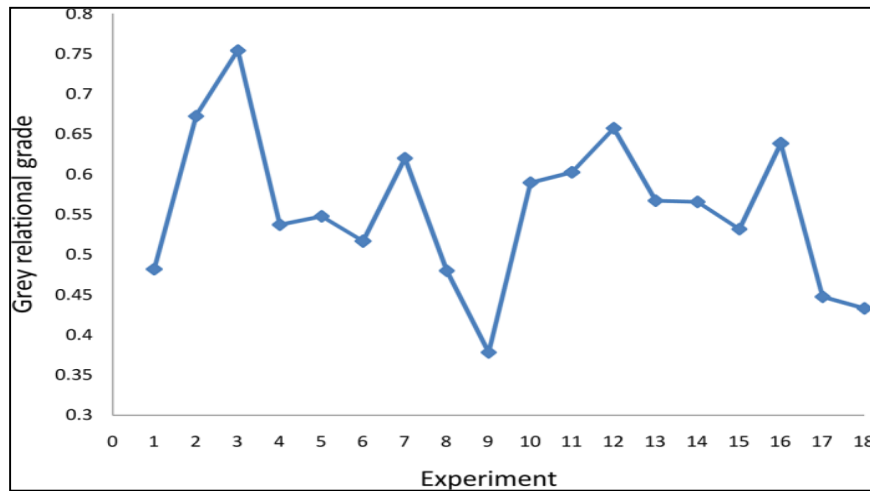


Fig. 5:

Considering the maximization of the grey rank values (Table 6 and Fig. 6), the optimal parameter conditions, A1B1C3D3 are obtained.

Symbol	Parameter	1	2	3	Optimum Level	Max-Min	Rank
A	Current	0.5888	0.5813	0.4744	1	0.1144	1
B	Pulse on time	0.6013	0.5038	0.5439	1	0.0975	2
C	Pulse off time	0.5456	0.5375	0.5598	3	0.0223	4
D	Dielectric pressure	0.5081	0.5524	0.5899	3	0.0818	3

Table 6: Performance table of the grey relation rank.

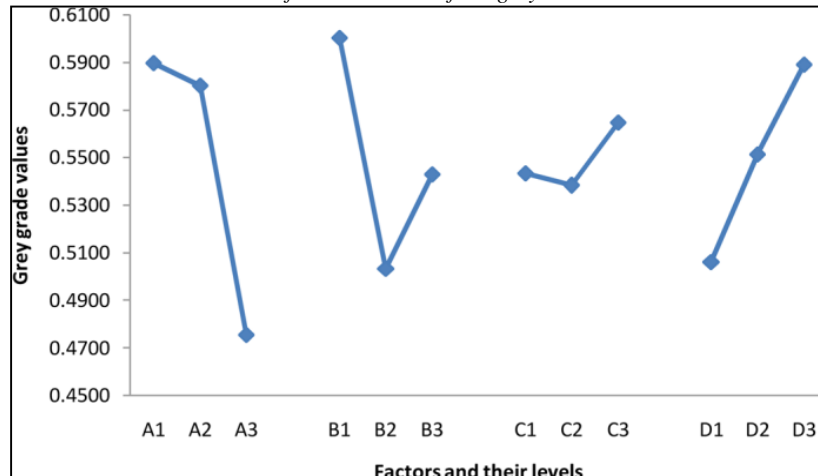


Fig. 6: Response graph of the grey relation rank.

ANOVA is performed to identify the significant parameters. This variance analysis is conducted by a static process that analyses the output in specific parameters. The output of the ANOVA determines the impact of the consequences on each parameter. The Taguchi method is incapable of scrutinizing the results for every parameter of the method; therefore, a particular percentage of the ANOVA is utilized to obtain a balanced outcome. When the F value is large, a change in the eroding parameters plays a vital role in the results. The ANOVA of the GRG is presented in Table 7. The current, pulse on time, and dielectric pressure are identified as significant parameters that affect the GRG in Fig. 7.

Symbol	Parameter	SS	DOF	MS	F-cal	% Contribution	Rank
A	Current	0.0464	2	0.0232	17.8500	33.50	1
B	Pulse on time	0.0389	2	0.0194	14.9230	28.08	2
C	Pulse off time	0.0039	2	0.0020	1.5385	3.00	4
D	Dielectric pressure	0.0379	2	0.0189	14.5400	27.34	3
Error		0.0114	9	0.0013		8.23	
Total		0.1385	17				

Table 7: Significance of the spark eroding parameters as obtained through ANOVA.

SS-Sum of Square, DOF-Degrees of freedom, MS-Mean Square, %-Percentage

	Machining Parameters in 2 trial	Optimal machining Parameter in 2 trial	
		Prediction	Experiment
Setting Level	A1B3C3D3	A1B1C3D3	A1B1C3D3
Material removal rate (g/min)	0.0185	-	0.0250
Tool wear rate(g/min)	0.0011	-	0.0010
Circularity (mm)	0.016	-	0.012
Dilation (mm)	0.028	-	0.015
Taper Ratio (mm)	0.214	-	0.210
Grey relational grade	0.7542	-	0.7675

Table 8: Results of the validation experiment.

Improvement of the Grey relational grade 0.0133

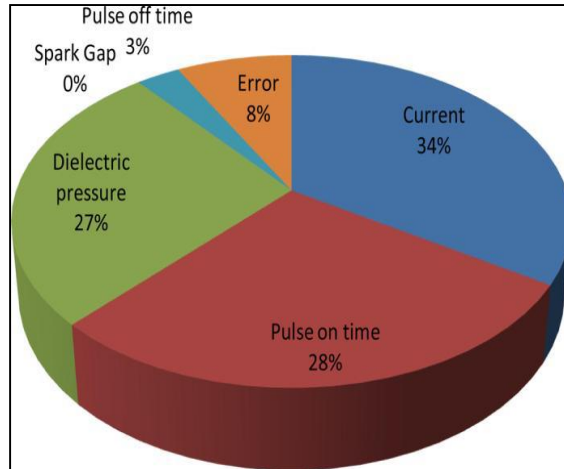


Fig. 7: Proportional values of the contributing factors by ANOVA

The optimum condition is computed. A selected optimum level of the input parameters to forecast and validate a confirmatory characteristic uses the ideal level of design parameters. The expected S/N ratio constitutes the ideal values of the design parameters.

$$\hat{\eta} = \eta_m + \sum_{i=1}^m (\eta_i - \eta_m) \dots \dots \dots (9)$$

In this equation, η_m = the average S/N ratio, η_i = the mean S/N ratio relating to the i^{th} important parameter on j^{th} level and q = number of important parameters.

The grey relational grade (GRG) is estimated by applying Equation (9), and the optimum combinations of the eroding parameters related to various response characteristics are determined. A validation experiment is executed using the spark EDM to verify and enhance the performance characteristics of ceramic composites. Furthermore, the GRG for several response optimizations completed in the spark eroding process is enhanced between 0.7542 and 0.7675. Therefore, the outcome is confirmed by the optimization of the EDM parameters using the GRA.

IV. CONCLUSIONS

This study proposes an optimization procedure for the spark eroding process of a SiC ceramic composite based on the GRA of the Taguchi method. The optimal process parameters are attained by the GRG for multi-response optimization.

- 1) Factor A (current), factor B (pulse on time) and factor E (dielectric pressure) contribute 33.50%, 28.08% and 27.34%, respectively, to the ANOVA. The above factors are recognized as the most significant parameters affecting the accuracy and precision of the spark EDM process.
- 2) The appropriate combination of the results is obtained by the factor level settings, A1B1C3D3, which resemble the 3rd experimental parametric combination.
- 3) Furthermore, this technique improves the target output performance parameters with relation to the MRR, TWR, Circularity (mm), Over cut(Dilation of hole), Taper Ratio by applying the optimum level of input parameters, such as the current (I), pulse on time (Ton), pulse off time (T off) and dielectric pressure (DP).
- 4) The experiment is conducted within the optimum settings and results in a significant improvement in this process. The verification experiment shows that the responses of the spark erosion process can be efficiently improved.

- 5) Micro features on SiC ceramic composite using conventional sink EDM is successfully achieved with the satisfied form quality.

REFERENCES

- [1] Bhaduri, D.; Kuar, A.S.; Sarkar, S.; Biswas, S.K.; Mitra, S. Electro discharge machining of titanium nitride-aluminium oxide composite for optimum process criteria yield. *Materials and Manufacturing Process* 2009, 24 (12), 1312-1320.
- [2] Ahmad, N.; Sueyoshi, H. Microstructure and mechanical properties of silicon nitride–titanium nitride composites prepared by spark plasma sintering. *Material Research Bulletin* 2011, 46 (3), 460-463.
- [3] Wei, C.; Zhao, L.; Hu, D.; Ni, J. Electrical discharge machining of ceramic matrix composites with ceramic fiber reinforcements. *International Journal of Advanced Manufacturing Technology* 2013, 64 (1-4), 187-194.
- [4] Jiang, D.; Vleugels, J.; Van der Biest, O.; Liu, W.D.; Verheyen, R.; Lauwers, B. Electrically conductive and wear resistant Si₃N₄-based composites with TiC_{0.5}N_{0.5} particles for electrical discharge machining. *Material Science Forum* 2005, 492, 27-32.
- [5] Ahmad, N.; Sueyoshi, H. Densification and Mechanical Properties of Electro conductive Si₃N₄ -Based Composites Prepared by Spark Plasma Sintering. *Sains Malaysiana* 2012, 41, 1005-1009.
- [6] Sanchez, J.A.; Cabanes, I.; de Lacalle, L.L.; Lamikiz, A. Development of optimum electro discharge machining technology for advanced ceramics. *International Journal of Advanced Manufacturing Technology* 2001, 18 (12), 897-905.
- [7] Puertas, I.; Luis, C.J. A study on the electrical discharge machining of conductive ceramics. *Journal of Materials Processing Technology* 2004, 153, 1033-1038.
- [8] Ahmad, N.; Sueyoshi, H. Properties of Si₃N₄–TiN composites fabricated by spark plasma sintering by using a mixture of Si₃N₄ and Ti powders. *Ceramics International* 2010, 36 (2), 491-496.
- [9] Drawin, S.; Justin, J.F. Advanced Lightweight Silicide and Nitride Based Materials for Turbo-Engine Applications. *Onera—the French Aerospace Lab Journal* 2011, 3, 1-13.
- [10] Muttamara, A.; Janmanee, P.; Fukuzawa, Y. A Study of Micro-EDM on Silicon Nitride Using Electrode Materials. *International Transaction Journal of Engineering, Management, & Applied Sciences & Technologies* 2010, 1 (1), 1-7.
- [11] Dey, S.; Roy, D.C. Experimental Study Using Different Tools/Electrodes EG Copper, Graphite on MRR of EDM Process and Selecting The Best One for Maximum MRR in Optimum Condition. *International Journal of Modern Engineering Research* 2013, 3 (3), 1263-1267.
- [12] Puertas, I.; Luis, C.J. Optimization of EDM conditions in the manufacturing process of B₄C and WC-Co conductive ceramics. *The International Journal of Advanced Manufacturing Technology* 2012, 59 (5-8), 575-582.
- [13] Singh, P.N.; Raghukandan, K.; Pai, B.C. Optimization by Grey relational analysis of EDM parameters on machining Al–10% SiCP composites. *Journal of Materials Processing Technology* 2004, 155, 1658-1661.
- [14] Chiabert, P.; Lombardi, F.; Orlando, M. Benefits of geometric dimensioning and tolerancing. *Journal of Materials Processing Technology* 1998, 78(1), 29-35.
- [15] Arockia Jaswin, M.; Mohan Lal, D. Optimization of the cryogenic treatment process for En 52 valve steel using the Grey-Taguchi method. *Materials and Manufacturing Processes* 2010, 25 (8), 842-850.
- [16] Vijay Kumar, M.; Singh Azad, M. Grey relational analysis of micro-EDM machining of Ti-6Al-4 V alloy. *Materials and Manufacturing Processes* 2012, 27, 973– 977.
- [17] Lin, Y.C.; Lee, H.S. Optimization of machining parameters using magnetic force-assisted EDM based on gray relational analysis. *The International Journal of Advanced Manufacturing Technology* 2009, 42 (11-12), 1052-1064.
- [18] Kumar, A.; Maheshwari, S.; Sharma, C.; Beri, N. A study of multi objective parametric optimization of silicon abrasive mixed electrical discharge machining of tool steel. *Materials and Manufacturing processes* 2010, 25(10), 1041-1047.
- [19] Baraskar, S.S.; Banwait, S.S.; Laroia, S.C. Multi objective optimization of electrical discharge machining process using a hybrid method. *Materials and Manufacturing Processes* 2013, 28 (4), 348–354.
- [20] Muthuramalingam, T.; Mohan, B. Influence of discharge current pulse on machinability in electrical discharge machining. *Materials and Manufacturing Processes* 2013, 28 (4), 375–380.
- [21] Souza, C. C.; Arencibia, R. V.; Costa, H. L.; Piratelli Filho, A. A contribution to the measurement of circularity and cylindricity deviations. In *ABCM Symposium Series in Mechatronics* 2012, 5, 791.
- [22] Selvarajan, L.; Narayanan, C. S.; Jeyapaul, R. Optimization of Process Parameters to Improve Form and Orientation Tolerances in EDM of MoSi₂-SiC Composites. *Materials and Manufacturing Processes* 2014, doi:10.1080/10426914.2014.962041.
- [23] Hyun-Kyu Yooa, Ji-HyeKoa, Kwang-Young Limb, WonTaeKwona,n, Young-Wook Kimb. Micro-electrical discharge machining characteristics of newly developed conductive SiC ceramic. *Ceramics International* 41(2015)3490–3496
- [24] Mustafa Ay & Ulaş Çaydaş & Ahmet Haşçalık. Optimization of micro-EDM drilling of inconel 718 Super alloy. *Int J Adv Manuf Technol* (2013) 66:1015–1023.DOI 10.1007/s00170-012-4385-8.
- [25] Krishna Kumar Saxenaa,n, Anand Suman Srivastava b, SanjayAgarwal b , Experimental investigation into the micro-EDM characteristics of conductive SiC , *Ceramics International* ,<http://dx.doi.org/10.1016/j.ceramint.2015.09.11>.